A Characterization of Cold Pools in the West African Sahel

Article *in* Monthly Weather Review · November 2015

DOI: 10.1175/MWR-D-15-0023.1

4 authors, including:

Miroslav Provod

6 PUBLICATIONS **9** CITATIONS

SEE PROFILE

John H. Marsham

University of Leeds

159 PUBLICATIONS **1,650** CITATIONS

SEE PROFILE

Douglas J. Parker

University of Leeds

110 PUBLICATIONS **3,262** CITATIONS

SEE PROFILE

A characterization of cold pools in the West African Sahel

Authors and their institutions:

[1]M Provod (University of Leeds), Email: eempr@leeds.ac.uk

Dr J H Marsham (Water @ Leeds, University of Leeds), Email: j.marsham@leeds.ac.uk

Prof D J Parker (University of Leeds), Email: d.j.parker@leeds.ac.uk

Dr Cathryn E Birch (Met Office @ Leeds), Email: cathryn.birch@metoffice.gov.uk

Institutional addresses:

School of Earth and Environment
The University of Leeds
Leeds, LS2 9JT
United Kingdom

[1] Corresponding author

Abstract

Cold pools are integral components of squall-line mesoscale convective systems and the West African Monsoon, but are poorly represented in operational global models. Observations of thirty-eight cold pools made at Niamey during the 2006 AMMA (African Monsoon Multidisciplinary Analysis) campaign (1 June to 30 September 2006), are used to generate a seasonal characterization of cold-pool properties by quantifying related changes in surface meteorological variables. Cold pools were associated with temperature decreases of 2 to 14°C, pressure increases of 0 to 8 hPa and wind gusts of 3 to 22 m s^{-1}. Comparison with published values of similar variables from the Great Plains of the USA showed comparable differences. The leading part of most cold pools had decreased water vapour mixing ratios compared to the environment, with moister air, likely related to precipitation, approximately 30 minutes behind the gust front. A novel diagnostic used to quantify how consistent observed cold pool temperatures are with saturated or unsaturated descent from mid-levels (Fractional Evaporational Energy Deficit, FEED) shows that early-season cold pools are consistent with less saturated descents. Early season cold pools were relatively colder, windier and wetter, consistent with drier mid-levels, although this was only statistically significant for the change in moisture. Late season cold pools tended to decrease equivalent potential temperature from the pre-cold-pool value, whereas earlier in the season changes were smaller, with more increases. The role of cold pools may therefore change through the season, with early season cold-pools more able to feed subsequent convection.

1. Introduction

Mesoscale convective systems (MCSs) form an integral part of the West African Monsoon (Flamant *et al*. 2007; Marsham *et al.* 2013a) and account for more than 80% of the annual rainfall in most of the Sahel (Mathon *et al.* 2002; Dhonneur, 1973). Cold pools produced by MCSs are important for a number of reasons; they are a key mechanism for maintenance of the MCSs, and for secondary initiation of new cumulonimbus systems; they transport substantial amounts of cold air northwards, cooling and moistening the Saharan heat-low by advection (Marsham *et al.* 2013; Garcia-Carreras *et al.* 2013), they are responsible for around 50% of summertime dust uplift in the Sahel & Sahara (Marsham *et al.* 2008; Marsham *et al.* 2011b; Heinold *et al.* 2013; Marsham *et al*. 2013b) and are associated with intense rain and strong winds.

In the summer, seasonally increasing south-westerly monsoon winds advect moist high equivalent potential temperature (Θ_e) low level air into the Sahel, which undercuts the dry mid-level Saharan Air Layer (SAL; Parker *et al.* 2005a). The SAL is characterised by almost

dry adiabatic lapse rates, which together with the low-level moisture results in large quantities of Convective Available Potential Energy (CAPE). There is, however, high Convective Inhibition (CIN), which together with mid-tropospheric dry air needs to be overcome for deep convection to be initiated and sustained.

Localised triggering initially creates discrete small-scale convective storms (Dione *et al.,* 2013) that can, under certain conditions, grow upscale to form an MCS, often in the form of a propagating squall line (Hamilton *et al.* 1945; Aspliden *et al.* 1976; Fortune, 1980; Chong *et al.* 1987; Lebel *et al*., 1997a, b; Futyan and Del Genio, 2007; Chong *et al.* 2010; Lafore *et al.* 2010; Lothon *et al.* 2011; Birch *et al*. 2013). Due to the presence of mid-tropospheric dry air masses in the Sahel, latent cooling caused by evaporation, melting or sublimation of hydrometeors is supportive of the formation of a cooler than environment downdraft (Redelsperger and Lafore, 1988). This cooler air then reaches the surface and spreads out as a density current – the cold pool (Charba, 1974; Mueller and Carbone, 1987). Together with the ambient wind shear, the cold pool helps to lift surrounding air parcels (e.g. Dione *et al.,* 2013) and create new cells, organizing the MCS (Roca *et al.* 2005). Therefore, cold pools play an important role in organizing deep moist convection and are an integral part of MCSs (Thorpe *et al.* 1982; Rotunno *et al.* 1988; Weisman *et al.* 1988*;* Fovell and Ogura 1989; Szeto and Cho 1994a, b; Trier *et al.* 1997; Parker and Johnson 2004a, b).

Perhaps the largest observational study of cold pool properties to date is based in the USA over Oklahoma and was performed by Engerer *et al.* (2008; hereafter E2008). Their study investigated 39 squall line MCSs by using data from 110 mesonet stations across the state of Oklahoma and obtained 1389 time series of cold pool related variables. The cold

pool quantities studied by E2008 were decreases in potential and equivalent potential temperature, pressure rises, changes in wind direction and maximum wind gusts. The focus of their study was on the evolution of cold pool properties during various life cycles of MCSs as well as comparison of the observed cold pool characteristics with idealised model simulations. Given that this study was based in the USA, it is of interest to assess whether the particular conditions of MCSs in West Africa result in comparable distributions of cold pool properties. As far as the authors are aware, there are several case studies of West-African MCSs (e.g. Chong *et al.* 2010; McGraw-Herdeg, 2010), but to date there is no general characterization of surface cold-pool properties.

This paper studies observed properties of West African cold pools produced by organized MCSs, mostly squall-lines, and compares them to results obtained in Oklahoma by E2008. One goal of this paper is to provide observational results for future studies to better evaluate cold pools in models. The monsoon season is split into three sub-periods to enable evaluation of seasonal evolution of MCS-related cold pool properties. Section 2 describes the observational data sets and the analysis method. Section 3*a* focuses on thermodynamic properties such as pressure and temperature and their seasonal variations. Section 3*b* studies cold-pool winds. Section 4 summarizes the results and discusses their implications.

2. Data and methods

a. Data

The African Monsoon Multidisciplinary Analysis Special Observing Period (AMMA SOP) took place in 2006. Documentation of MCSs was one of the key components of AMMA and the data obtained during AMMA currently provide the most detailed and complete dataset for moist convection in West Africa (Redelsperger *et al.* 2006, Lebel et al. 2010).

The MIT (Massachusetts Institute of Technology) C-Band Doppler radar was deployed near Niamey, Niger (13.5° N, 2.2°E) during AMMA. Scans were recorded at 10-minute intervals during the AMMA Radar Observing Period (AMMA ROP), which ran from 5 July 2006 until 27 September 2006. For the purpose of this study we used 360° long-range (250 km) surveys at 0.7° elevation in addition to Meteosat infrared satellite images.

The ARM (Atmospheric Radiation Measurement) Climate Research mobile facility was deployed at Niamey airport. Surface meteorology data obtained from this station were used in this study. The surface data consist of pressure, temperature, relative humidity, 10-m winds and rainfall intensity. For the purpose of this study, these data were used to calculate surface equivalent potential temperature and Water Vapour Mixing Ratio (WVMR). These were available in minute-averaged intervals for the whole AMMA SOP.

Radiosondes were released daily from Niamey airport approximately 30 minutes before 00, 06, 12 and 18 UTC. Some days had additional radiosonde releases approximately 30 minutes before 03, 09, 15 and 21 UTC. Local time is identical to UTC time (with solar noon at 11:57 UTC on 15 July 2006). There were, however, days when radiosonde ascents

were missing or delayed.

b. Method

The study period spanned from 1st June to 30th September 2006. A very similar approach to E2008 has been applied to allow comparison between West African MCS cold pools and E2008's results from the USA. E2008 subjectively identified cold-pool crossing times and then objectively quantified changes in surface station variables from the 30 minutes preceding the cold pool crossing to the two hours subsequent to the crossing. The 30 minute time window used to detect pre-storm maxima and minima in surface variables used by E2008 was not always long enough to capture these in Niamey, mainly in case of pressure as the pre-storm minimum was on average 52 minutes ahead of the cold pool. Therefore, in this study, the pre-storm time window was extended to 1 hour before the cold pool arrival time.

Time series of surface station data for an example cold pool, observed on 11th August 2006 at Niamey Airport, are shown in Figure 1. Cold pool crossings are associated with a sudden change in wind direction (Engerer *et al.* 2008; Fujita, 1963) and as in E2008 the wind direction change was considered as the main factor in the identification of crossing times (e.g. Figure 1). Times of sudden wind direction changes were subjectively identified and counted as potential cold pools. In order for the wind direction change to be sudden, it must have happened within 5 minutes and been of at least 30-degree magnitude. Because a wind direction change may, however, be associated with features other than cold pools (e.g.

209 dust devils (Tratt *et al.,* 2003), or gravity waves (Cram *et al., 1992,* Birch *et al.,* 2013)), the
210 other surface variables were also considered as specified below.
211
212 The change in wind direction must have occurred within 30 minutes of a wind gust
213 and changes in temperature and pressure to be counted as cold-pool related. The
214 magnitude of the gust must have been at least 1.5 times greater than the mean wind speed
215 in the 30 minutes before the gust and temperature must have dropped by at least 1°C (e.g.
216 Figure 1). It is not likely, but possible, that something other than an MCS cold pool in the Sahel
217 would cause these changes in pressure, temperature and wind. Because of this limitation of
218 using surface data only, all the identified cold pools were verified by considering images
219 from the MIT radar or satellite (outside of the ROP). This verification has been done
220 subjectively based on inspection of radar/satellite images to see whether an MCS has been
221 present in the vicinity of Niamey at the time of the cold pool passage.
222
223 Following the approach of E2008, the cold pool related changes in surface variables
224 were calculated for: (1) increase in pressure (the maximum after the cold-pool minus the
225 minimum before), and (2) decrease in temperature (maximum before minus the minimum
226 after). For (3) equivalent potential temperature (Θ_e), cold pools could give an increase or a
227 decrease, and often short-lived fluctuations complicated any method based on minima and
228 maxima; therefore, unlike E2008, changes in mean from the period spanning 1 hour before
229 the cold-pool crossing-time to the period spanning 2 hours after the crossing were
230 calculated. In addition, unlike E2008, (4) change in water vapour mixing ratio (WVMR) and
231 (5) increase in mean wind speed were also calculated. For WVMR, the mean value in the
232 hour before the cold pool was subtracted from the minimum value in the 2 hours after (so

positive values show moistening). The minimum after the passage was used rather than maximum as there was often a sharp minimum just following a cold pool passage, that was often followed by an increase that reached greater than pre-cold pool magnitudes within the 2 hours, but which was likely not primarily related to the cold pool crossing (e.g. Figure 1). The mean value in the 1 hour before the cold pool was used rather than a maximum in order to take into account the sometimes sharp fluctuations in WVMR that were likely related to turbulence and mixing. In addition, maximum wind gust associated with the cold pool was obtained by taking maximum wind speed in the 2 hours after the cold pool crossing (as in E2008).

For a majority of the studied cold pools, the cold-pool-related changes in surface variables were coincident or nearly coincident. There were, however, several cases where this was not the case and hence it was difficult to define the cold pool crossing time. This was most frequent in case of wind-direction changes, where in several cases there were multiple wind-direction changes of more than 30° within ~2 hours of a wind gust, but none coincided with the actual wind gust. These were likely related to waves propagating faster than the cold pool from the parent storm. In such cases either the time of the closest wind direction change to the gust or the time of the actual gust was taken as the crossing time, based on whichever was closest to the temperature drop. Because of this there is clearly uncertainty in the cold pool crossing times, but E2008 show the objectively determined changes are generally robust to the precise crossing time used.

Using the radar and Meteosat imagery, the storms generating the cold pools were separated subjectively into isolated storms and larger organized convective systems (MCSs;

257 spanning at least 100km as defined by American Meteorological Society, 2014). The main
258 difference between the methods of E2008 and this study is that MCS lifecycle stage
259 differentiation was not used because there was one radar available in the Sahel, which is
260 not enough information to decide on the lifecycle stage as it covers only a fraction of the
261 MCSs lifecycle. Instead, data were separated by sub-periods.
262
263 It was hypothesised that cold pool intensity would depend on mid-level dryness.
264 Therefore, the whole season was divided into three sub-periods based on the seasonal
265 evolution of rainfall at Niamey (Figure 2). We refer to these sub-periods as: "Pre-monsoon"
266 (1st June 2006 – 12th July 2006), "Monsoon" (13th July 2006 – 27th August 2006) and
267 "Retreat" (27th August 2006 – 30th September 2006), although they are not based on any
268 formal definition of monsoon onset. The sub-period boundaries were set based on
269 subjectively-identified changes of slope in the observed time-series of accumulated rainfall
270 (clearest for pre-monsoon to monsoon). Out of the 38 cold pools used in this study, 22
271 occurred in the 'monsoon' sub-period with 8 in the 'pre-monsoon' and 8 in the 'retreat' sub-
272 periods.
273
274
275 **3. Results and discussion**
276
277 During the study period, 42 cold pools were detected. Of these, 33 were squall-line
278 MCSs (having a continuous line being at least 100 km in length and having reflectivity of at
279 least 35 dBz along at least 50% of its length), 4 were non-squall-line MCSs, one was a
280 propagating cold pool from a freshly dissipated MCS (seen in satellite imagery but out of

281 radar range) and 4 were from local non-MCS convection (there were many isolated
282 convective storms in the range of the MIT radar, but their cold pools rarely crossed Niamey).
283 The 4 cold pools related to the isolated convection gave very limited statistics and since this
284 study focuses on cold pools produced by organised MCS's, data from these 4 cases were not
285 used in the analysis.
286
287 Figure 3 shows composites of surface variables, centred on cold pool crossing time.
288 The "composite cold pool", (over the entire observation period, black lines), was
289 accompanied by a decrease in temperature of 5.3°C. As expected, the cooling of the cold
290 pool brings a pressure increase, the magnitude of which was 1.9 hPa. The wind maximum
291 related to the cold pool passage had a magnitude of 6.5 m s^{-1} in the composite, with the
292 wind rotating from approximately 200 to 120 degrees. Rainfall intensity increased rapidly to
293 a maximum about 15 minutes after the cold pool passage with a second peak approximately
294 45 minutes after the passage. The weaker precipitation behind the first peak corresponds to
295 the "weak echo" in the radar observations, between stratiform rain and the main line of
296 convective cells. WVMR decreased after the initial passage and stayed low throughout the
297 first "convective rainfall" maximum. Approximately 30 minutes after the cold pool passage,
298 there was a small increase of WVMR (accompanied by an increase in relative humidity, not
299 shown). Although only around 0.5 g kg^{-1} this change is approximately twice the standard
300 error in the composite of cold-pool changes (not shown) and this temporary decrease
301 followed by an increase was observed in 26 out of 38 cases. The increase was coincident
302 with the second "stratiform" rainfall peak. This drying and moistening coincidence with the
303 rainfall suggests that there may be a descent of dry mid-level air towards the surface
304 occurring during the convective rainfall occurrence, while later evaporation of stratiform

305 rain increases WVMR.

306

307 Figure 3 shows that cold-pool related changes are different across the sub-periods.
308 Pre-monsoon cold pools are associated with greater pressure increases, temperature
309 decreases, less intense and shorter-lived precipitation and stronger winds. Furthermore, the
310 related changes in equivalent potential temperature and WVMR vary. The statistical
311 significance of these seasonal differences is investigated in later sections. All values given
312 below are means and standard deviations. The composite pre-monsoon cold pools caused a
313 long-lived WVMR increase of 2.5 g kg^{-1} ± 0.8 g kg^{-1}, while during the monsoon and retreat
314 there are long-lived decreases of 1.5 ± 0.2 and 2.7 ± 0.5 g kg^{-1} respectively. Equivalent
315 potential temperature changes very little with a pre-monsoon cold pool passage. In
316 contrast, there is a sharp and long-lived decrease in equivalent potential temperature in the
317 monsoon and retreat sub-periods, with the decrease during the retreat being greater than
318 during the monsoon (11.9 ± 10°C and 7.8 ± 4 8°C respectively). The rainfall structure of pre-
319 monsoon MCSs also appears to be different: the two rainfall peaks are less clear and later
320 stratiform rain makes a smaller contribution to the total.

321

322 ***a) Thermodynamic properties of cold pools***

323

324 Figure 4 shows bar plots of the normalised frequency distribution of several cold
325 pool properties and their seasonal variations. The bars are normalized to allow comparison
326 between sub-seasons and account for the different numbers of cold pools identified in the
327 three sub-periods. There were 8 events each in “pre-monsoon” and “retreat” and 22 in
328 “monsoon”; therefore “monsoon” was normalised by multiplying the number of events by

329 8/22 to allow comparison. The black line which shows the frequency distribution over all
330 three sub-periods therefore only overlies the top of the bar plots when there are no
331 “monsoon” events in that bin. .
332
333 A temperature decrease between 1.8 ˚C and 13.1 ˚C was observed for all cold pool
334 passages (Figure 4a). The whole seasonal distribution is skewed however, with a broad peak
335 between approximately 3 ˚C and 7 ˚C and only 3 events of temperature decrease greater
336 than 11 ˚C. The distribution of pressure increase in Figure 4b is also skewed, ranging from
337 0.4 to 7.6 hPa, with most events between 1 and 4 hPa. These values are larger than the
338 pressure increase in the cold pool composite in Figure 3 because the timing of the maximum
339 and minimum pressure relative to the gust-front differs between cold pools. This is a
340 limitation of the composite as minima and maxima occur at relatively different times from
341 the time of crossing; partly because cold pools propagate at different speeds and also
342 because for any system the maxima/minima are located at different positions relative to the
343 gust front.
344
345 Figure 4c shows that the majority of cold pools led to a drying, but 10 cold pools
346 (27%) led to an increase in WVMR. The WVMR increase ranged from -3.4 g kg^{-1} to +6.1 gkg^{-1}.
347 Most events gave a decrease in mean Θ_e with the greatest decrease being -12.6 ˚C but
348 several events show an increase, with the largest being +8.7 ˚C (Figure 4d). Bar plots of
349 relative humidity are not shown, but it was found that all cold pools gave increases in RH of
350 magnitudes between 0 and 60%. It was found that the three cold pools with greatest WVMR
351 increases were closest to rain, but no overall relationship could be concluded between the
352 WVMR change and its proximity to rainfall.

353

354 There was a tendency towards greater pressure increases and temperature
355 decreases in the pre-monsoon period when compared to the whole season (mean changes
356 were 3.4 hPa for pre-monsoon compared to 2.9 hPa overall and 7.8 ˚C compared with
357 5.9 ˚C overall). The differences in pressure and temperature changes between sub-seasons
358 were, however, not statistically significant at the 90% level. Humidity changes from cold
359 pools also varied across the sub-periods, with WVMR tending to increase in pre-monsoon,
360 but tending to decrease in the rest of the season (means of +1.1 g kg^{-1} for pre-monsoon
361 compared with -0.6 gkg^{-1} overall). Mean equivalent potential temperature both increased
362 and decreased in the pre-monsoon, but nearly always decreased in the remainder of the
363 observation period (mean changes of -2.2˚C compared with -9.6 ˚C). The seasonal
364 differences in changes equivalent potential temperature and WVMR were significant at the
365 90% level. This pre-monsoon difference is consistent with drier mid-levels during the pre-
366 monsoon period that promote more evaporation (or sublimation) and hence greater
367 associated moistening, cooling and greater pressure increases, although the differences
368 were only statistically significant for the moistening (see also section 3a 1). It is also
369 consistent with Garcia-Carreras, *et al.* (2013) who shows that cold pools carry moisture
370 northwards into the Sahara from the Sahel during the pre-monsoon period.
371

372 Figures 5a and 5b show that colder cold pools give larger pressure increases, as
373 expected. This relationship is most consistent for pre-monsoon cases, which have a
374 correlation of 0.6 (statistically significant at $p<0.11$), with monsoon and retreat periods
375 having only weak correlations of 0.08 and -0.2 respectively (not statistically significant). The
376 overall correlation for the season was 0.3 (statistically significant at $p<0.07$).

The overall distribution in Figure 5a is similar to that shown in Figure 5 of E2008, except that a small percentage of cold pools in Engerer's study (1.5%) had either larger pressure increases or temperature deficits. Based on the total number of data points and the data points with temperature decrease greater than 14 °C or pressure increase greater than 7 hPa in E2008, we would expect approximately 0.6 data-points with magnitudes of at least 14 °C or 7 hPa for temperature decrease and pressure increase respectively to be found in our study if magnitudes of cold pool properties in Niamey were identical to those in Oklahoma. The fact that there were no such cold pools in our study, however, is not statistically significant at the 0.05 significance level to conclude that cold pools in Niamey are weaker in terms of temperature decrease and pressure increase when compared to Oklahoma. A considerably larger data-set would be needed to make any conclusions about the occurrence of such strong cold pools in Niamey when compared to Oklahoma. Note that MCSs tend to be observed at a particular point in their lifecycle in Niamey. This was often either in a mature or dissipating stage, although difficult to differentiate at times due to only one radar data source and attenuation by rainfall as already discussed. Hence, stronger cold pools may be observed elsewhere in West Africa. This is a limitation of this observational study, which was, by necessity, confined to one spatial point.

Observed night-time cold pools are generally associated with higher values of pressure increase for a given temperature decrease than day-time ones (Figure 5b). The reason for this is likely the fact that at night the boundary layer tends to be stable due to nocturnal cooling and during the day the surface layer is unstable. The magnitude of the cold pool related change in temperature aloft is therefore greater than observed at the

surface at night, and less during the day (Davies *et al.* 2005). The cold pool may also slide on top of the stably stratified surface layer at night (Heinold *et al.* 2013; Marsham 2011a), significantly reducing the temperature decrease measured at the surface. However, both small and large decreases in surface temperature in Figure 5b show that at least some of downdrafts at Niamey routinely reach the surface despite the presence of a nocturnal inversion. Figure 5b shows that pressure increases greater than ~5 hPa occurred only at night or in the morning (before 8am), which is consistent with E2008 and likely the result of deeper cold pools associated with maturing/dissipating MCSs and the known tendency for large organised systems at night over Niamey (Rickenbach *et al.* 2009).

1) Role of mid-level dryness

It was hypothesised that the stronger cold pools in the pre-monsoon period (with greater wind gusts, see section 3*b*) may be caused by seasonally drier mid-levels in that period (Marsham *et al*. 2008; Barnes and Sieckman 1984). We test this hypothesis using a one-dimensional conceptual model, where radiosonde data were used to quantify mid-level dryness for each cold pool using Θ_w (wet-bulb potential temperature) depression (i.e. difference between Θ and Θ_w averaged between 550 and 750 hPa) using the nearest pre-storm sounding. These soundings were between 38 minutes and 5 hours 52 minutes before the cold pool crossing. Despite the long gaps between the radio-sounding and the cold pool in some cases, these were the best mid-level data available. In reality, the applicability of the one-dimensional model may be limited by significant horizontal gradients and transports; this may in future be tested in high-resolution modelling studies.

Figure 6 shows how close observed cold pool temperatures are to idealised descents

425 of mid-level air. In this figure, we plot “departure from moist adiabat” (DMA), defined as

426 $$DMA = \Theta_{cold\ pool} - mean\ (\Theta_{w\ (550\ to\ 750\ hPa)})$$

427 Against mid-level dryness defined using the difference between mean potential
428 temperature and wet-bulb potential temperature in the 550 to 750 hPa layer. Therefore Fig.
429 6 shows how the cold pool potential temperature minus the wet-bulb potential
430 temperature of mid-levels (y-axis) depends on the mid-level Θ_w depression. If mid-level air
431 was cooled by evaporation of precipitation and descended whilst being kept saturated by
432 continued evaporation then the air would descend moist adiabatically and the cold pool
433 potential temperature would equal the mid-level Θ_w (y-axis value equals zero in Fig. 6). In
434 contrast, if mid-level air instead descended completely dry-adiabatically then the potential
435 temperature of the cold pool would equal the potential temperature of the mid-levels and
436 data would lie on the one-to-one line in Fig. 6. Therefore, how far the data are from the
437 one-to-one towards the x-axis line in Fig. 6 is a measure of the degree of saturation in the
438 idealised one-dimensional descent. We therefore refer to the y-axis as the “Departure from
439 Moist Adiabat” (DMA) and the ratio of both axes as the “Fractional Evaporational Energy
440 Deficit” (FEED), with the one-to-one line of FEED = 100%.

441

442 The values in Figure 6 can also be related to the energetics of the downdraught. For
443 a fixed pressure of source air, the potential energy of cooling by evaporation is
444 approximately proportional to the x-axis value (the energy is proportional to the tephigram-
445 area bounded by the Θ_w line of saturated descending air and the theta-line for unsaturated
446 descending air, and here we approximate this by a triangle). As noted above, if FEED is zero,
447 then the downdraught is fully saturated in its descent, and we could regard DCAPE
448 (Downdraft Convective Available Potential Energy) to be a good measure of the

449 downdraught potential energy released.

450

451 Figure 6 shows that $\Theta_{cold\ pool}$ values are never equal to mid-level Θ_w values, with the
452 moistest cold pool having DMA of 3.6 °C, confirming that no cold pool in our study was
453 formed by the theoretical, perfectly moist adiabatic descent of mid-level air. In contrast, the
454 highest value of DMA is 16.1 °C. All data points lie below the line of FEED of 67% and the
455 lowest data point has a FEED of 17.6%. The overall relationship suggests that drier mid-
456 levels are related to greater DMA and FEED (correlation between DMA and mid-level Θ_w
457 depression is 0.5 with $p < 0.001$, correlation between FEED and mid-level Θ_w depression is
458 0.03 with $p < 0.89$). This suggests that the ability of precipitation to keep the descending
459 parcel saturated decreases with drier mid-levels, which may be due to greater mixing of dry
460 air or insufficient availability of precipitation to be evaporated into the descending parcel.
461 Pre-monsoon data points have generally greater percentages of FEED and lie closer to the
462 FEED of 67% line. This is not statistically significant, but suggests that the drier atmosphere
463 in the pre-monsoon period may lead to drier descents.

464

465 ***b) Cold-pool winds***

466

467 The observed maximum wind gusts range from 4 to 22 ms^{-1} with most cold pools
468 having gusts between 2.5 and 12.5 m s^{-1} (Figure 7a). The mean wind can either increase (26
469 cases) or decrease (11 cases) during a cold pool passage, with the magnitudes of increase
470 generally between 0 and 6 ms^{-1}, with the greatest value of increase being ~10 ms^{-1} (Figure
471 7b). The magnitudes of the decreases were less than 3 ms^{-1} and were always associated with
472 a mean decrease of the general environmental wind speed.

The mean for maximum wind gusts in the pre-monsoon period was 10.1 ms^{-1}, which was greater than that in the monsoon and retreat periods (7.6 and 7.5ms^{-1} respectively). This difference was, however, not statistically significant. There were comparable mean wind-speed changes (+1.4, +1.6 and +1.4 for pre-monsoon, monsoon and retreat respectively). The mean pre-monsoon gusts were strongly affected by a single strong event on 17th June, when the highest gust of 21.4 ms^{-1} was recorded. If this case was removed then the mean pre-monsoon gust decrease to 8.5 ms^{-1}(still higher than other sub-periods, but again not significantly).

The relation between pressure changes and maximum wind gusts, which are partly driven by the pressure changes, has a correlation of 0.46 ($p < 0.004$ – statistically significant) (Figure 8). There was one outlier (the 17th June event), where additional features such as mixing of momentum from upper levels may have caused stronger winds than would be expected from the observed pressure increase alone. If this outlier is taken away, the correlation reduces to 0.42 ($p < 0.01$, still statistically significant). The diurnal distribution of cold pool related wind gusts shows that the higher cold-pool related gusts (above ~10 ms^{-1}) weren't limited to the daytime. This contradicts the fact that the stably stratified nocturnal boundary layer can inhibit cold-pool winds at night (Parker 2008; Marsham *et al.* 2011a); cold pools over Niamey from some of the mature nocturnal MCSs can clearly mix down through this night-time stable layer (see also temperature changes in section 3*a*).

4. Conclusions

MCSs are an important feature of the West African Monsoon, providing most of the rainfall over the Sahel. Cold pools contribute to the organisation of these MCSs, form a crucial component of the monsoon flow (Marsham *et al.* 2013) and ventilate the Saharan heat low (Garcia-Carreras *et al.* 2013). This study has quantified properties of cold pools from MCSs observed over Niamey in the Sahel during the 2006 AMMA field campaign, using a methodology similar to E2008.

Every observed cold pool in this study was associated with a temperature decrease, ranging from 1.8 ˚C to 13.6 ˚C, and a pressure increase, ranging from 0.4 hPa to 8.1hPa. These observed ranges generally agree with those observed by E2008 in the USA, but are missing E2008's largest values. Given the much smaller sample size of our study, it is not possible to say whether these more intense events are rarer in Niamey than the USA or whether our sample is too small to observe them.

Water vapour mixing ratio was found to decrease just after the cold pool passage in all but 9 cases. The magnitude of the decrease did not exceed 3.4 g kg^{-1}. This initial decrease was in many cases followed by an increase in the mixing ratio of around 0.5 g kg^{-1}, sometimes to values greater than before the cold pool passage, which appears to be generated by the MCS rainfall. The mean equivalent potential temperature was found to increase in 6 out of the 38 cases, but decrease in others. A maximum in observed winds has been identified with every passage of an MCS, ranging from 3.7 ms^{-1} to 21.6 ms^{-1}. The time-averaged 10-m mean wind from before to after the gust front was found to usually increase, although decreases were observed, with changes ranging from -2.3 to +10.0 ms^{-1}.

Cold pools in the pre-monsoon period gave larger pressure increases and temperature decreases, as well as larger maximum wind gusts and mean wind increases, when compared to the monsoon and retreat periods. These were, however, not statistically significant. Pre-monsoon cold pools increased rather than decreased WVMR. Pre-monsoon cases gave little overall change in equivalent potential temperature, which tended to be decreased by cold pools in the monsoon and retreat periods. These differences in changes in WVMR and Θ_e between cold pools during the pre-monsoon and later periods were statistically significant at the 90% significance level. Furthermore, we define the Departure from Moist Adiabat (DMA) and Fractional Evaporational Energy Deficit (FEED) and use a simple 1D model to quantify how close the observed cold pools were near wet adiabatic (FEED=0%) or dry adiabatic (FEED=100%) descent. FEED varied from 17.6% to 64.5%, with drier descents for drier mid-levels and during the pre-monsoon period (with only a correlation of 0.5 between DMA and mid-level Θ_w depression). The importance of cold pools in the Sahel suggests that future studies should use AMMA observations to evaluate modelled cold pools in operational and research models. Such evaluations could make use of DMA and FEED as defined here, which would be strengthened by trajectory analyses from a high-resolution model.

The results show that early season cold pools provide high equivalent potential temperature air at low levels, which especially if reheated could feed later convection, once the high CIN is overcome (see also Torri *et al.,* 2015). Later in the season, the cold pools reduce equivalent potential temperature but will still favor convection by lifting. The results are consistent with observations from Garcia-Carreras *et al.* (2013), who show that cold

pools bring moist air towards the Saharan heat low early in the season. The results support the hypothesis that early in the monsoon season, when mid-levels are drier and there is therefore greater diabatic cooling, cold pools will make a greater contribution to the monsoon flow (Marsham *et al.,* 2013).

Acknowledgements

We would like to thank all the reviewers for their constructive and helpful comments. Surface meteorological data were obtained from the ARM Climate Research Facility (U.S. Department of Energy) deployed in Niamey in the AMMA campaign. Based on a French initiative, AMMA (http://www.amma-international.org) was built by an international group. MIT radar was made available to AMMA from Massachusetts Institute of Technology. AMMA-UK has been funded by NERC grants NE/B505538/1 and NE/G018499/1. Thanks to Richard Pope and many others for practical help with using data analysis software.

References

Aspliden, C. I., 1976: Classification of Structure of Tropical Atmosphere and Related Energy Fluxes. *J. App. Meteor.,* ***15***, 692-697.

Barnes, G. M., and Sieckman, K., 1984: The Environment of Fast-Moving and Slow-Moving Tropical Mesoscale Convective Cloud Lines. *Mon. Wea. Rev.,* ***112***, 1782-1794.

Birch, C. E., D. J. Parker, A. O'Leary, C. M. Taylor, J. H. Marsham, P. Harris and G. Lister, 2013: The impact of soil moisture and atmospheric waves on the development of a mesoscale convective system: A model study of an observed AMMA case, *Q. J. R.*

570 *Meteor. Soc.*, **139**, 1712-1730.

571 Charba, J., 1974: Application of Gravity Current Model to Analysis of Squall-Line Gust Front.
572 *Mon. Wea. Rev., **102***, 140-156.
573 Chong, M., Amayenc, P., Scialom, G., and Testud, J., 1987: A Tropical Squall Line Observed
574 during the Copt-81 Experiment in West-Africa .1. Kinematic Structure Inferred from
575 Dual-Doppler Radar Data. *Mon. Wea. Rev., **115***, 670-694.

576 Chong, M., 2010: The 11 August 2006 squall-line system as observed from MIT Doppler
577 radar during the AMMA SOP. *Q. J. R. Meteor. Soc., **136***, 209-226.

578 Cram, J. M., Pielke, R. A., and Cotton and W. R., 1992: Numerical-Simulation and Analysis of
579 a Prefrontal Squall Line .2. Propagation of the Squall Line as an Internal Gravity-
580 Wave. *J. Atmos. Sci., **49***, 209-225.
581 Davies, T., Cullen, M. J. P., Malcolm, A. J., Mawson, M. H., Staniforth, A., White, A. A., &
582 Wood, N., 2005: A new dynamical core for the Met Office's global and regional
583 modelling of the atmosphere. *Q. J. R. Meteor. Soc.,* **131**(608), 1759-1782.
584 Dhonneur, G., 1973: Study of a Line Squall in Niger Bend. *Bull. Amer. Meteor. Soc., **54***, 1075-
585 1075.
586 Dione, C., M. Lothon, D. Badiane, B. Campistron, F. Couvreux, F. Guichard, and S. Salle,
587 2013: Phenomenology of Sahelian convection observed in Niamey during the
588 early monsoon. *Q. J. R. Meteor. Soc.,* **140**, 500-516.
589 Dixon, N. S., Parker, D. J., Taylor, C. M., Garcia-Carreras, L., Harris, P. P., Marsham, J. H., and
590 Woolley, A., 2013: The effect of background wind on mesoscale circulations above
591 variable soil moisture in the Sahel *Q. J. R. Meteor. Soc., **139***, 1009-1024.

592 Engerer, N. A., Stensrud, D. J., and Coniglio, M. C., 2008: Surface Characteristics of Observed
593 Cold Pools. *Mon. Wea. Rev., **136***, 4839-4849.
594 Flamant, C., Chaboureau, J. P., Parker, D. J., Taylor, C. A., Cammas, J. P., Bock, O. Pelon, J.,
595 2007: Airborne observations of the impact of a convective system on the planetary
596 boundary layer thermodynamics and aerosol distribution in the inter-tropical
597 discontinuity region of the West African Monsoon. *Q. J. R. Meteor. Soc., **133***, 1175-
598 1189.
599 Fortune, M., 1980: Properties of African Squall Lines Inferred from Time-Lapse Satellite
600 Imagery. *Mon. Wea. Rev., **108***, 153-168.
601 Fovell, R. G., and Ogura, Y., 1989: Effect of Vertical Wind Shear on Numerically Simulated
602 Multicell Storm Structure. *J. Atmos. Sci., **46***, 3144-3176.
603 Fujita, T., 1963: Precise Reduction of Radiation Data from Meteorological Satellites. *J. Opt.*
604 *Soc. America, **53***, 1331-&.
605 Futyan, J. M., and Del Genio, A. D., 2007: Deep convective system evolution over Africa and
606 the tropical Atlantic. *J. Climate, **20***, 5041-5060.
607 Garcia-Carreras, L., Marsham, J. H., Parker, D. J., Bain, C. L., Milton, S., Saci and A.
608 Washington, R., 2013: The impact of convective cold pool outflows on model biases
609 in the Sahara. *Geo. Res. Lett., **40***, 1647-1652.
610 Hamilton, R. A., and Archbold, J. W., 1945: Meteorology of Nigeria and Adjacent Territory. *Q.*
611 *J. R. Meteor. Soc., **71***, 231-&.
612 Heinold, B., Knippertz, P., Marsham, J. H., Fiedler, S., Dixon, N. S., Schepanski and K.Tegen, I.,
613 2013: The role of deep convection and nocturnal low-level jets for dust emission in
614 summertime West Africa: Estimates from convection-permitting simulations. *J. Geo.*
615 *Res. Atmos., **118***, 4385-4400.

Lafore, J. P., Redelsperger, J. L., and Jaubert, G., 1988: Comparison between a 3-Dimensional Simulation and Doppler Radar Data of a Tropical Squall Line - Transports of Mass, Momentum, Heat, and Moisture. *J. Atmos. Sci., **45***, 3483-3500.

Lebel, T., Taupin, J. D., and D'Amato, N., 1997a: Rainfall monitoring during HAPEX-Sahel .1. General rainfall conditions and climatology. *J. Hyd., **189***, 74-96.

Lebel, T., and LeBarbe, L., 1997b: Rainfall monitoring during HAPEX-Sahel .2. Point and areal estimation at the event and seasonal scales. *J. Hyd., **189***, 97-122.

Lothon, M., Campistron, B., Chong, M., Couvreux, F., Guichard, F., Rio, C., and Williams, E., 2011: Life Cycle of a Mesoscale Circular Gust Front Observed by a C-Band Doppler Radar in West Africa. *Mon. Wea. Rev., **139***, 1370-1388.

Marsham, J. H., Dixon, N. S., Garcia-Carreras, L., Lister, G. M. S., Parker, D. J., Knippertz, P., and Birch, C. E., 2013a: The role of moist convection in the West African monsoon system: Insights from continental-scale convection-permitting simulations. *Geo. Res. Lett., **40***, 1843-1849.

Marsham, J. H., Hobby, M., Allen, C. J. T., Banks, J. R., Bart, M., Brooks, B. J., and Washington, R., 2013b: Meteorology and dust in the central Sahara: Observations from Fennec supersite-1 during the June 2011 Intensive Observation Period. *J. Geo. Res. Atmos., **118***, 4069-4089.

Marsham, J. H., Trier, S. B., Weckwerth, T. M., and Wilson J. W., 2011a: Observations of Elevated Convection Initiation Leading to a Surface-Based Squall Line during 13 June IHOP_2002. *Mon. Wea. Rev., **139***, 247-271.

Marsham, J. H., Knippertz, P., Dixon, N. S., Parker, D. J., and Lister, G. M. S., 2011b: The importance of the representation of deep convection for modelled dust-generating winds over West Africa during summer. *Geo. Res. Lett., **38***.

Marsham, J. H., Parker, D. J., Grams, C. M., Taylor, C. M., and Haywood, J. M., 2008: Uplift of Saharan dust south of the intertropical discontinuity. *J. Geo. Res. Atmos., **113***

Mathon, V., Laurent, H., and Lebel, T., 2002: Mesoscale convective system rainfall in the Sahel. *J. App. Meteor., **41***, 1081-1092.

McGraw-Herdeg, M., 2010: Dusty gust fronts and their contributions to long-lived convection in West Africa. Ph.D. thesis, Department of Electrical Engineering and Computer Science.

Mueller, C. K., and Carbone, R. E., 1987: Dynamics of a Thunderstorm Outflow. *J. Atmos. Sci., **44***, 1879-1898.

Parker, M. D., and Johnson, R. H., 2004a: Simulated convective lines with leading precipitation. Part I: Governing dynamics. *J. Atmos. Sci., **61***, 1637-1655.

Parker, M. D., and Johnson, R. H., 2004b: Simulated convective lines with leading precipitation. Part II: Evolution and maintenance. *J. Atmos. Sci., **61***, 1656-1673.

Parker, DJ, Thorncroft CD, Burton RR, Diongue-Niang A., 2005a: Analysis of the African easterly jet, using aircraft observations from the JET2000 experiment, Q.J.R. *Meteor. Soc., **131**, 1461-1482.*

Parker, M.D., 2008: Response of simulated squall lines to low-level cooling. *J. Atmos. Sci.*, **65**, 1323-1341.

Redelsperger, J. L., and Lafore, J. P., 1988: A 3-Dimensional Simulation of a Tropical Squall Line - Convective Organization and Thermodynamic Vertical Transport. *J. Atmos. Sci., **45***, 1334-1356.

Redelsperger, J. L., Thorncroft, C. D., Diedhiou, A., Lebel, T., Parker, D. J., and Polcher, J., 2006: African monsoon multidisciplinary analysis - An international research project and field campaign. *Bull. Amer. Meteor. Soc., **87***, 1739-+.

Rickenbach, T., Ferreira, R. N., Guy, N., and Williams, E., 2009: Radar-observed squall line propagation and the diurnal cycle of convection in Niamey, Niger, during the 2006 African Monsoon and Multidisciplinary Analyses Intensive Observing Period. *J. Geo. Res. Atmos.,* ***114***.

Roca, R., Louvet, S., Picon, L., and Desbois, M., 2005: A study of convective systems, water vapour and top of the atmosphere cloud radiative forcing over the Indian Ocean using INSAT-1B and ERBE data. *Meteor. and Atmos. Phys.,* ***90***, 49-65.

Rotunno, R., Klemp, J. B., and Weisman, M. L., 1988: A Theory for Strong, Long-Lived Squall Lines. *J. Atmos. Sci.,* ***45***, 463-485.

Szeto, K. K., and Cho, H. R., 1994a: A Numerical Investigation of Squall Lines .1. The Control Experiment. *J. Atmos. Sci.,* ***51***, 414-424

Szeto, K. K., and Cho, H. R., 1994b: A Numerical Investigation of Squall Lines .2. The Mechanics of Evolution. *J. Atmos. Sci.,* ***51***, 425-433.

Taylor, C. M., Harding, R. J., Thorpe, A. J., and Bessemoulin, P., 1997: A mesoscale simulation of land surface heterogeneity from HAPEX-Sahel. *J. Hyd.,* ***189***, 1040-1066.

Thorpe, A. J., Miller, M. J., and Moncrieff, M. W., 1982: Two-Dimensional Convection in Non-Constant Shear - a Model of Mid-Latitude Squall Lines. *Q. J. R. Meteor. Soc.,* ***108***, 739-762.

Torri, G., Kuang Z., and Tian Y., 2015: Mechanisms for convection triggering by cold pools. *Geo. Res. Lett.*

Tratt, D. M., Hecht, M. H., Catling, D. C., Samulon, E. C., and Smith, P. H., 2003: In situ measurement of dust devil dynamics: Toward a strategy for Mars. *J. Geo. Res. Plan.,* ***108***.

Trier, S. B., Skamarock, W. C., and LeMone, M. A., 1997: Structure and evolution of the 22

February 1993 TOGA COARE squall line: Organization mechanisms inferred from numerical simulation. *J. Atmos. Sci.,* ***54***, 386-407.

Weisman, M. L. and J. B. Klemp *et al*., 1988: Structure and Evolution of Numerically Simulated Squall Lines. *J. Atmos. Sci.* **45**(14): 1990-2013.

List of Figures

Figure 1: *An example of an observed daily time series as obtained by the surface station at Niamey airport. This time series is for 11th August 2006, when a cold pool crossing was identified at 03:15 Local Time (denoted by vertical red line). Black lines denote the borders of the time-windows used for the analysis. Solid lines correspond to left-hand axis and dashed lines to right-hand axes. Data recorded every second and averaged at minute intervals.*

Figure 2: *Total accumulated rainfall from Niamey ARM surface station data. Red lines separate three seasonal periods used in this study: "Pre-monsoon" (1st June 2006 – 12th July 2006);"Monsoon" (13th July 2006 – 27th August 2006);"Retreat" (27th August 2006 – 30st September 2006).*

Figure 3: *Composite cold pools obtained from averaging variables of all cold pools around the crossing time. Black line is for the whole period, red for the Pre-Monsoon period, blue for the Monsoon and green for Retreat. The vertical pink line shows the cold pool crossing time.*

Figure 4: *Changes in specified thermodynamic variables from cold pools: a) Decrease in temperature; b) Increase in pressure; c) Increase in WVMR; d) Increase in mean* Θ_e. *Colouring represents the sub-periods (red: Pre-monsoon, blue: Monsoon, green: Retreat). Number of events in each season is normalised to allow a comparsion between seasons (see text) with the black line showing total (unnormalised) distributions.*

Figure 5 *Pressure increases and temperature decreases from cold pools. Colouring in (a) represents the whole period and sub-periods as in Figure 3. Colouring in (b) represents the time of day (red: 8 – 16 UTC, blue: 18 – 6 UTC, green: 6-8 UTC, there were no events between 16 and 18 UTC).*

Figure 6: *Departure from Moist Adiabat (DMA) which equals ($\Theta_{cold\ pool}$ – mean ($\Theta_{w\ (550\ to\ 750\ hPa)}$)) versus mid-level dryness defined using the difference between mean ($\Theta_{(550\ to\ 750\ hPa)}$) and mean ($\Theta_{w\ (550\ to\ 750\ hPa)}$). Colouring of points represents the sub-periods as in Figure 3. Diagonal lines represent constant Fractional Evaporational Energy Deficit (FEED) of 100% (black), 67% (blue) and 33% (red).*

Figure 7: *As Figure 4, but for (a) 10m wind gusts and (b) mean wind increases.*

Figure 8: *Cold pool pressure increases and maximum wind gusts. Colours represent different times of day (red: 8-17 UTC, blue: 19-6 UTC, green: 6-8 UTC, no cold pool crossed between 17-19 UTC).*

Figures

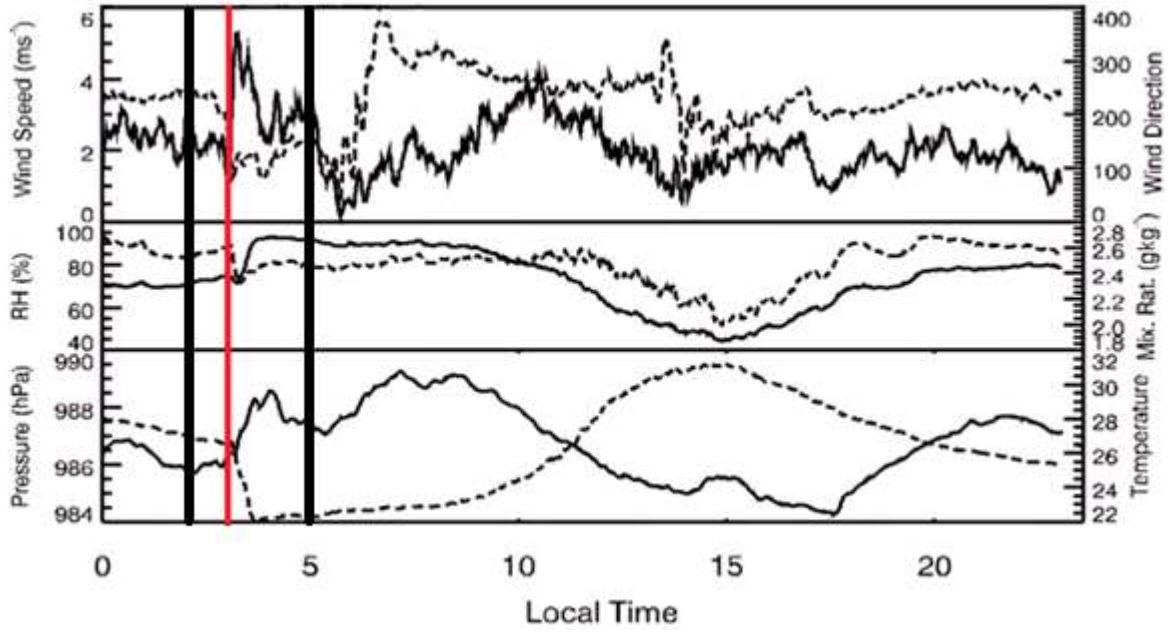

Figure 1: *An example of an observed daily time series as obtained by the surface station at Niamey airport. This time series is for 11th August 2006, when a cold pool crossing was identified at 03:15 Local Time (denoted by vertical red line). Black lines denote the borders of the time-windows used for the analysis. Solid lines correspond to left-hand axis and dashed lines to right-hand axes. Data recorded every second and averaged at minute intervals.*

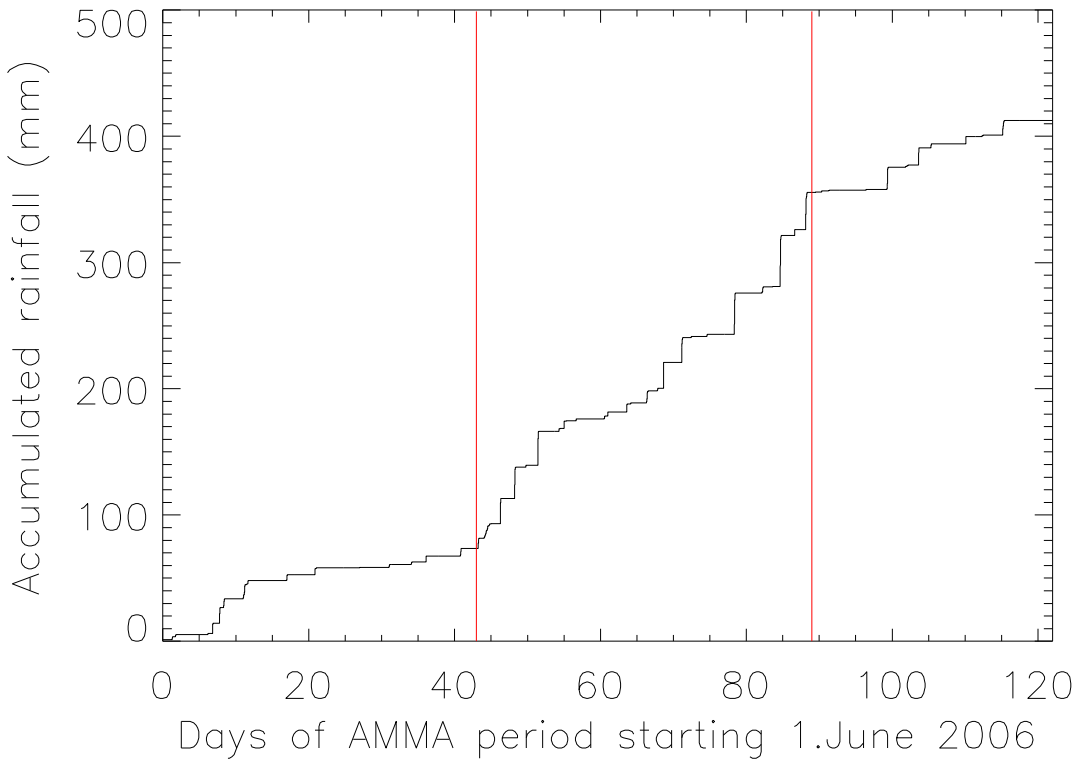

745

746 ***Figure 2:*** *Total accumulated rainfall from Niamey ARM surface station data. Red lines*

747 *separate three seasonal periods used in this study: "Pre-monsoon" (1st June 2006 – 12th July*

748 *2006);"Monsoon" (13th July 2006 – 27th August 2006);"Retreat" (27th August 2006 – 30st*

749 *September 2006).*

750

751

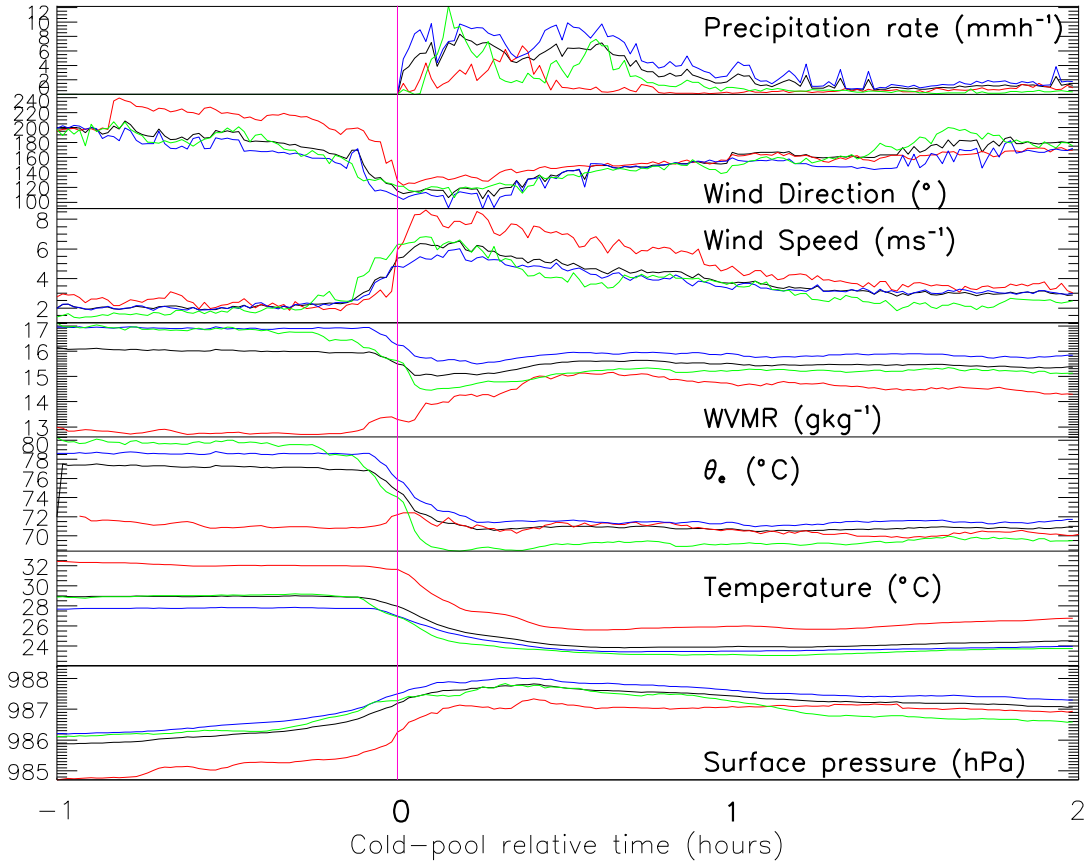

752

753 ***Figure 3:*** *Composite cold pools obtained from averaging variables of all cold pools around*

754 *the crossing time. Black line is for the whole period, red for the Pre-Monsoon period, blue for*

755 *the Monsoon and green for Retreat. The vertical pink line shows the cold pool crossing time.*

756

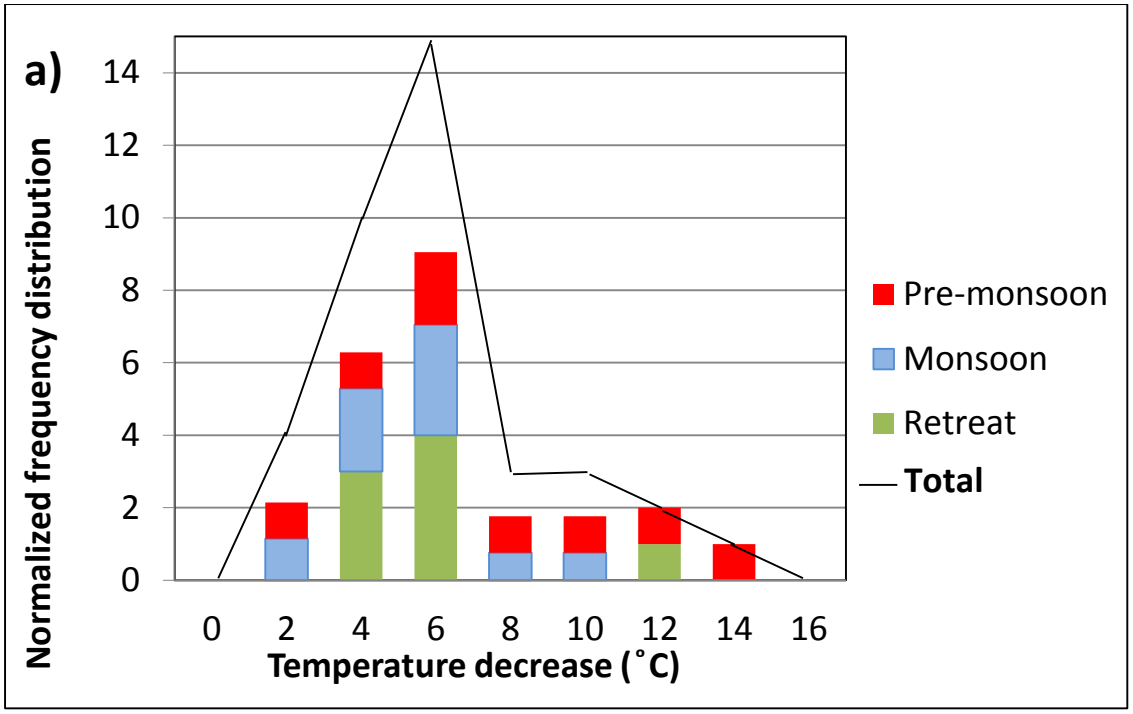
a)
Normalized frequency distribution
14
12
10
8
6
4
2
0
0 2 4 6 8 10 12 14 16
Temperature decrease (˚C)
Pre-monsoon
Monsoon
Retreat
Total

757

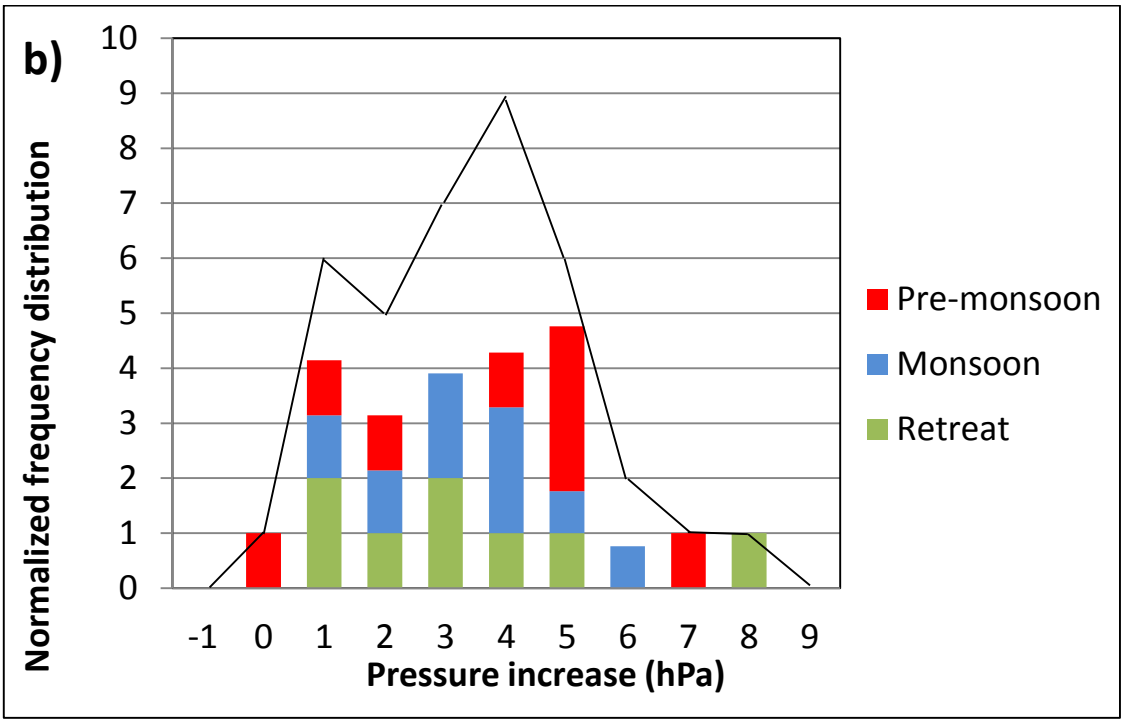
b)
Normalized frequency distribution
10
9
8
7
6
5
4
3
2
1
0
-1 0 1 2 3 4 5 6 7 8 9
Pressure increase (hPa)
Pre-monsoon
Monsoon
Retreat

758

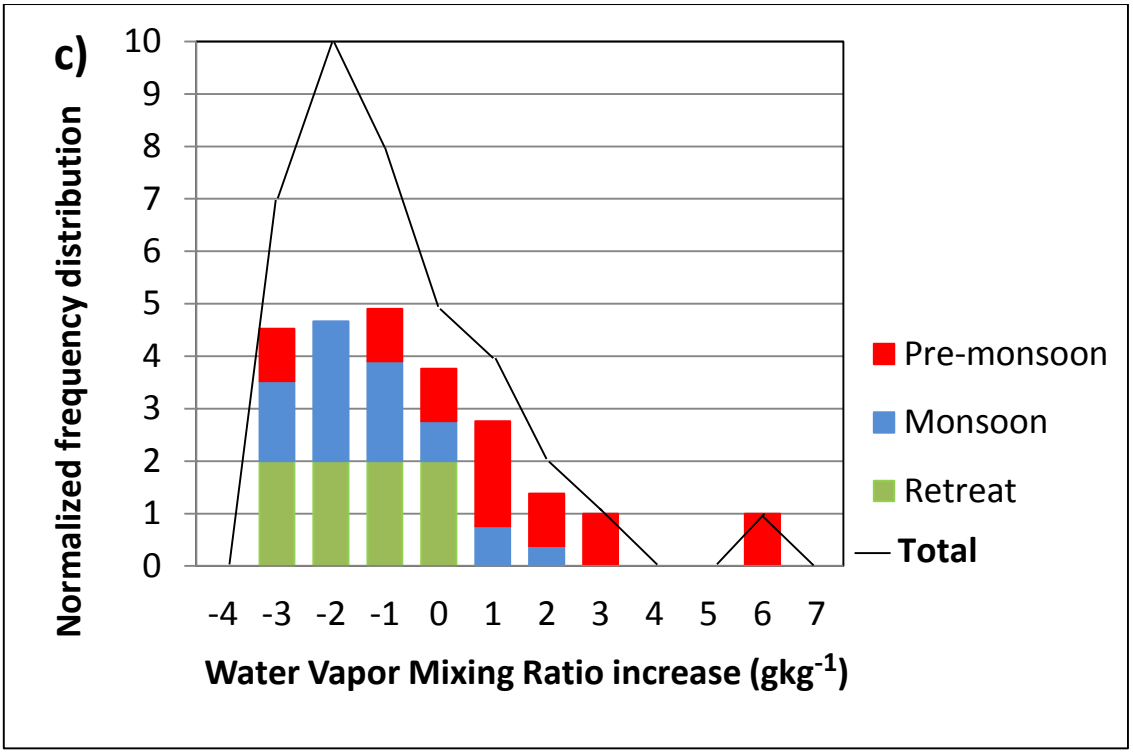

759

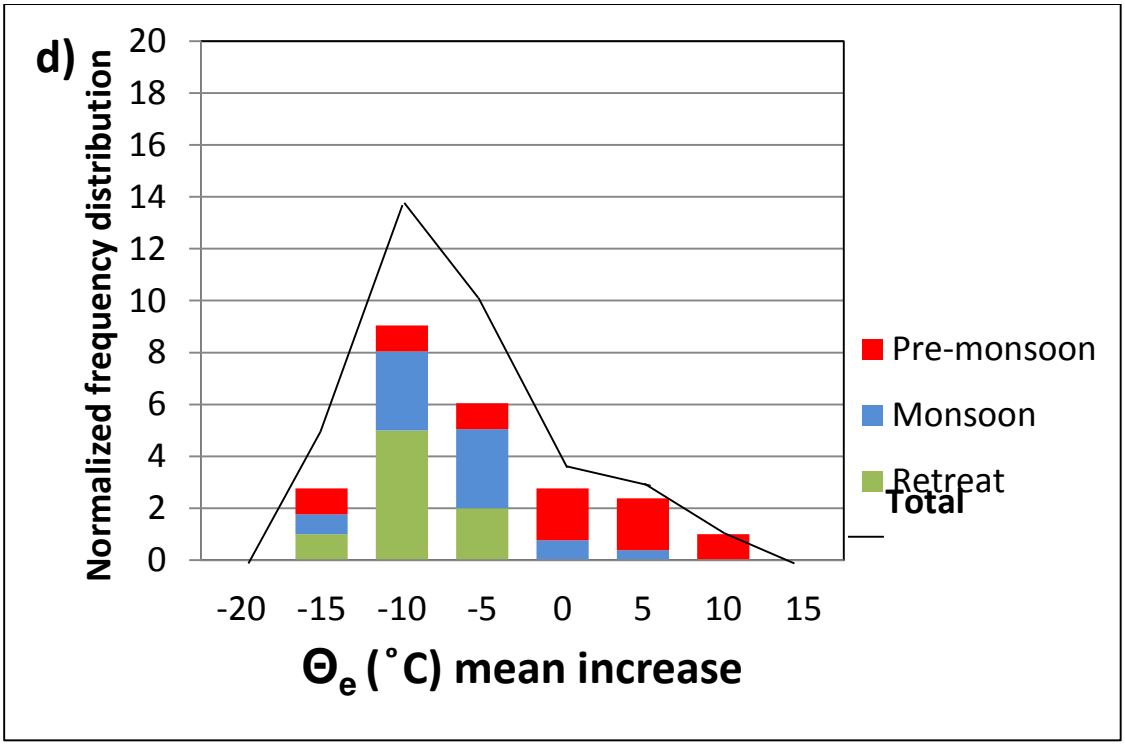

760

761 ***Figure 4:*** *Changes in specified thermodynamic variables from cold pools: a) Decrease in*

762 *temperature; b) Increase in pressure; c) Increase in WVMR; d) Increase in mean* Θ_e.

763 *Colouring represents the sub-periods (red: Pre-monsoon, blue: Monsoon, green: Retreat).*

764 *Number of events in each season is normalised to allow a comparsion between seasons (see*

text) with the black line showing total (unnormalised) distributions.

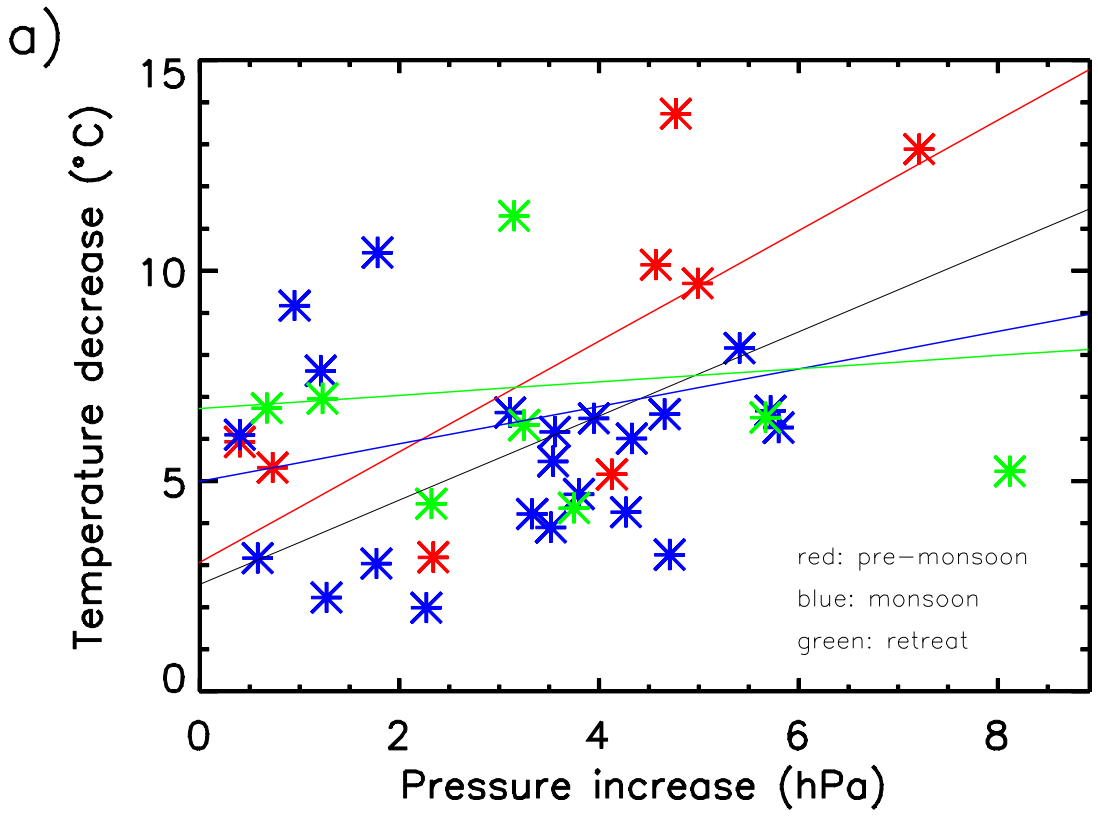

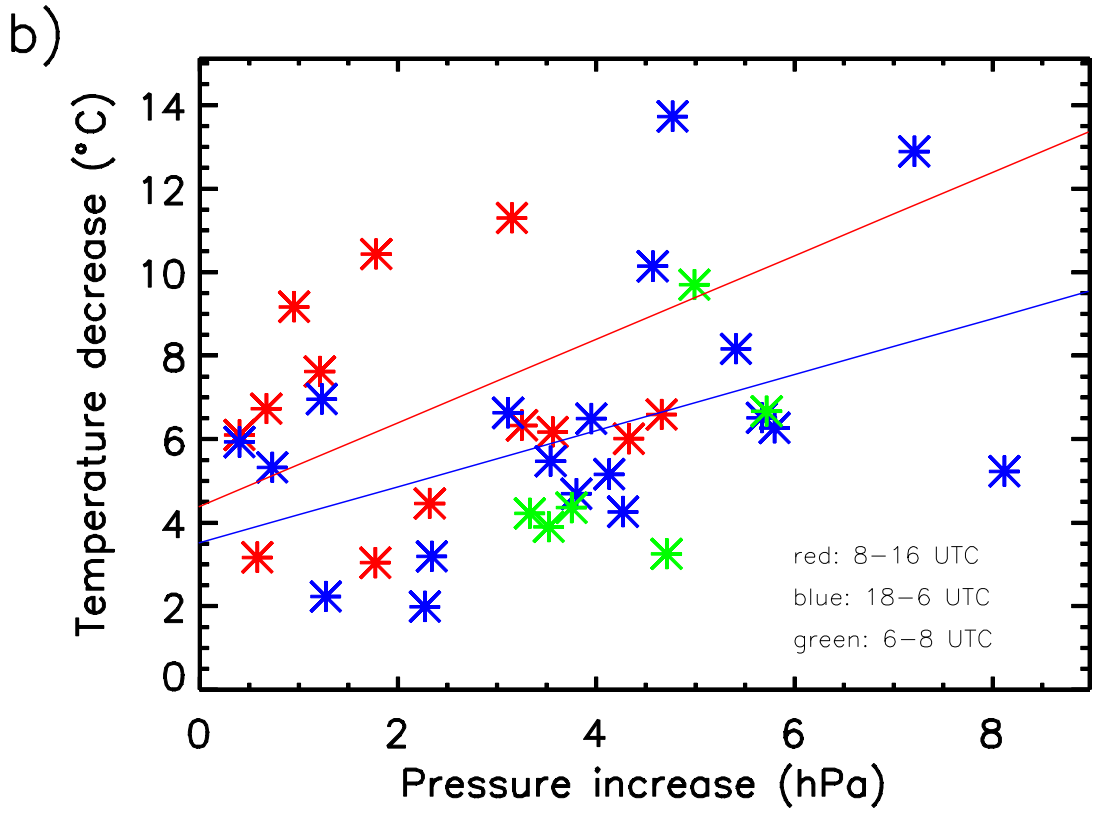

Figure 5 *Pressure increases and temperature decreases from cold pools. Colouring in (a) represents the whole period and sub-periods as in Figure 3. Colouring in (b) represents the time of day (red: 8 – 16 UTC, blue: 18 – 6 UTC, green: 6-8 UTC, there were no events between 16 and 18 UTC).*

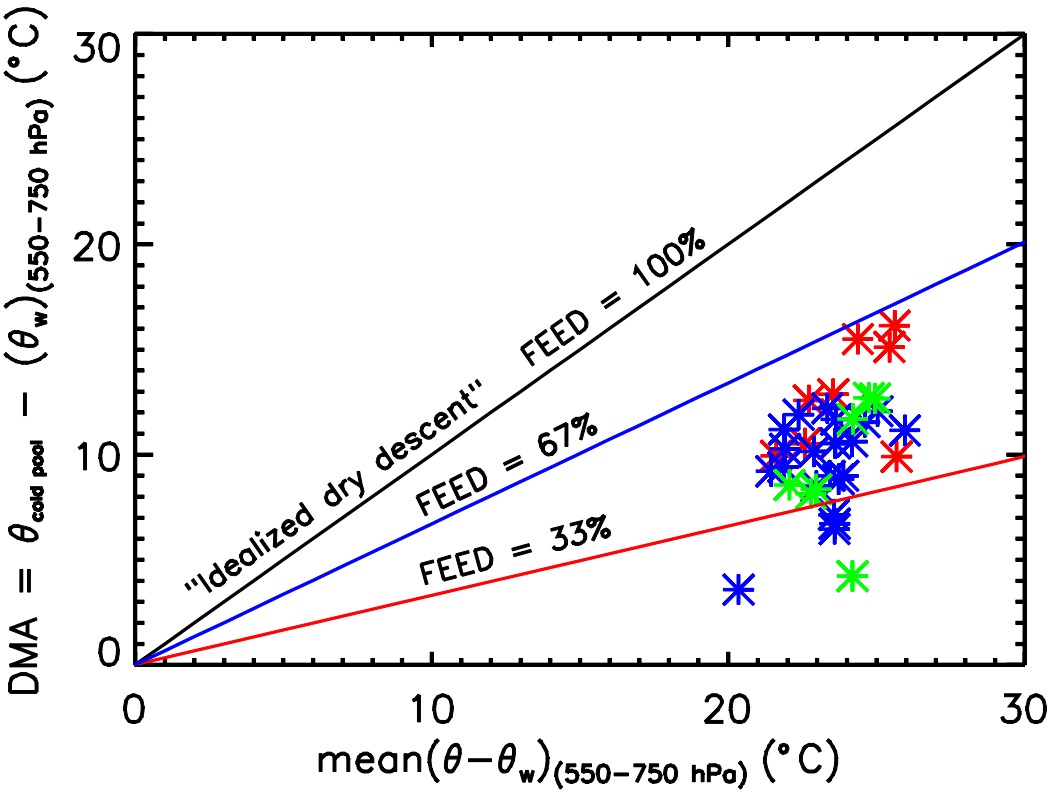

Figure 6: *Departure from Moist Adiabat (DMA = $\Theta_{cold\ pool}$ – mean ($\Theta_{w\ (550\ to\ 750\ hPa)}$)) versus mid-level dryness defined using the difference between mean ($\Theta_{(550\ to\ 750\ hPa)}$) and mean ($\Theta_{w\ (550\ to\ 750\ hPa)}$). Colouring of points represents the sub-periods as in Figure 3. Diagonal lines represent constant Fractional Evaporational Energy Deficit (FEED) of 100% (black), 67% (blue) and 33% (red).*

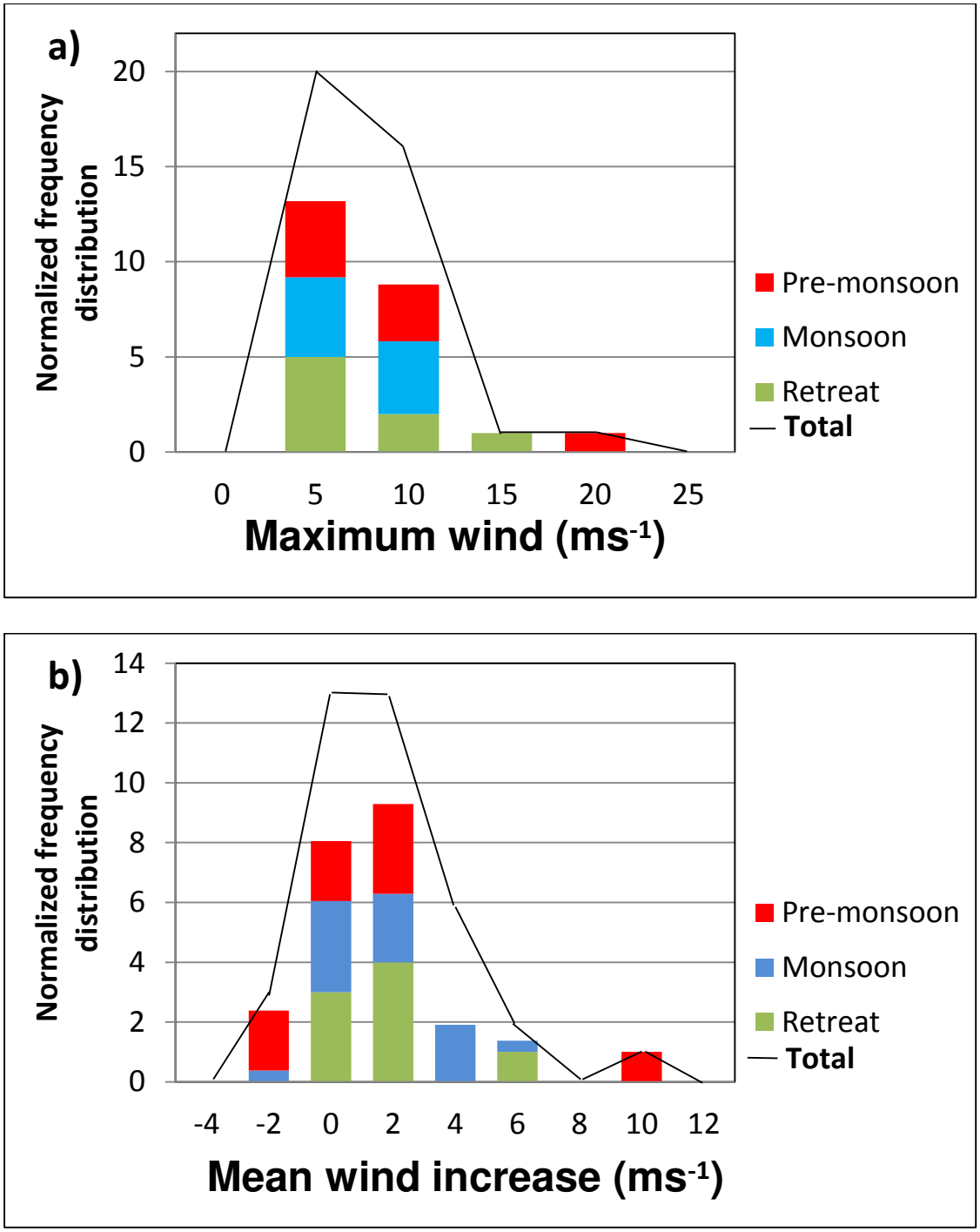

780

781

782

783 ***Figure 7:*** *As Figure 4, but for (a) 10m wind gusts and (b) mean wind increases.*

784

785

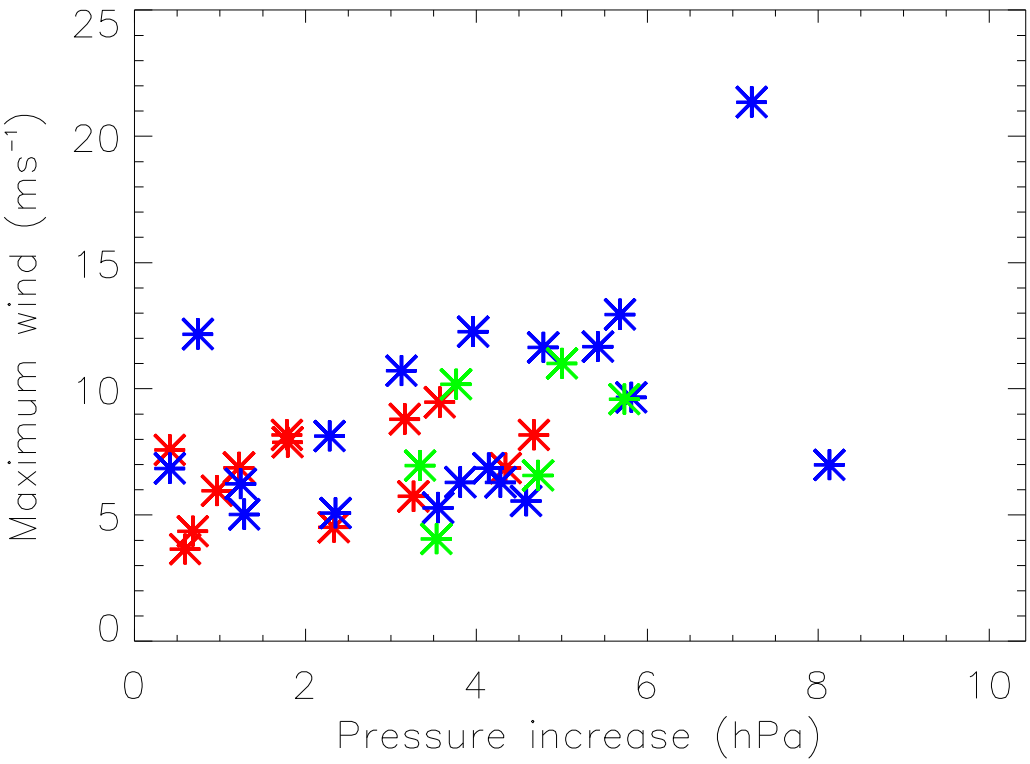

786

787 ***Figure 8:*** *Cold pool pressure increases and maximum wind gusts. Colours represent different*

788 *times of day (red: 8-17 UTC, blue: 19-6 UTC, green: 6-8 UTC, no cold pool crossed between*

789 *17-19 UTC).*

Non-Rendered Figure 1

Click here to download Non-Rendered Figure: Figure1.png

Non-Rendered Figure 2
Click here to download Non-Rendered Figure: Figure2.png

Non-Rendered Figure 3

Click here to download Non-Rendered Figure: Figure3.png

Non-Rendered Figure 4a
Click here to download Non-Rendered Figure: Figure4a.png

Non-Rendered Figure 4b
Click here to download Non-Rendered Figure: Figure4b.png

Non-Rendered Figure 4c
Click here to download Non-Rendered Figure: Figure4c.png

Non-Rendered Figure 4d

Click here to download Non-Rendered Figure: Figure4d.png

Non-Rendered Figure 5a
Click here to download Non-Rendered Figure: Figure5a.png

Non-Rendered Figure 5b
Click here to download Non-Rendered Figure: Figure5b.png

Non-Rendered Figure 6
Click here to download Non-Rendered Figure: Figure6.png

Non-Rendered Figure 7a
Click here to download Non-Rendered Figure: Figure7a.png

Non-Rendered Figure 7b
Click here to download Non-Rendered Figure: Figure7b.png

Non-Rendered Figure 8
Click here to download Non-Rendered Figure: Figure8.png